Published in final edited form as:
Invest Ophthalmol Vis Sci. 2005 July ; 46(7): 2540–2551.

Loss of Circadian Photoentrainment and Abnormal Retinal Electrophysiology in *Math5* Mutant Mice

Joseph A. Brzezinski IV[1,2,3], **Nadean L. Brown**[4,5,3], **Atsuhiro Tanikawa**[6], **Ronald A. Bush**[6], **Paul A. Sieving**[6,7], **Martha H. Vitaterna**[8], **Joseph S. Takahashi**[8,9], and **Tom Glaser**[1,2]
1 *From the Departments of Human Genetics and*

2*Internal Medicine, University of Michigan, Ann Arbor, Michigan; the*

4*Divisions of Developmental Biology and*

5*Ophthalmology, Children's Hospital Research Foundation, Department of Pediatrics, University of Cincinnati Medical School, Cincinnati, Ohio;*

6*Section for Translational Research on Retinal and Macular Degeneration, National Institute on Deafness and Other Communication Disorders, Bethesda, Maryland;*

7*National Eye Institute, Bethesda, Maryland;*

8*Center for Functional Genomics, Northwestern University, Evanston, Illinois; and the*

9*Department of Neurobiology and Physiology, Howard Hughes Medical Institute, Northwestern University, Evanston, Illinois.*

Abstract

Purpose—To determine how the absence of retinal ganglion cells (RGCs) in *Math5* (*Atoh7*) mutant mice affects circadian behavior and retinal function.

Methods—The wheel-running behavior of wild-type and *Math5* mutant mice was measured under various light–dark cycle conditions. To evaluate retinal input to the suprachiasmatic nuclei (SCN) anatomically, the retinohypothalamic tracts were labeled in vivo. To assess changes in retinal function, corneal flash electroretinograms (ERGs) from mutant and wild-type mice were compared under dark- and light-adapted conditions. Alterations in retinal neuron populations were evaluated quantitatively and with cell-type–specific markers.

Results—The *Math5*-null mice did not entrain to light and exhibited free-running circadian behavior with a mean period (23.6 ± 0.15 hours) that was indistinguishable from that of wild-type mice (23.4 ± 0.19 hours). The SCN showed no anterograde labeling with a horseradish peroxidase–conjugated cholera toxin B (CT-HRP) tracer. ERGs recorded from mutant mice had diminished scotopic a- and b-wave and photopic b-wave amplitudes. The scotopic b-wave was more severely affected than the a-wave. The oscillatory potentials (OPs) and scotopic threshold response (STR) were also reduced. Consistent with these ERG findings, a pan-specific reduction in the number of bipolar cells and a smaller relative decrease in the number of rods in mutant mice were observed.

Conclusions—*Math5*-null mice are clock-blind and have no RGC projections to the SCN. RGCs are thus essential for photoentrainment in mice, but are not necessary for the development or intrinsic

Corresponding author: Tom Glaser, Departments of Internal Medicine and Human Genetics, The University of Michigan, 1150 W. Medical Center Drive, 4520 MSRB I Box 0651, Ann Arbor, MI 48109; tglaser@umich.edu..
[3]Contributed equally to the work and therefore should be considered equivalent authors.

This work was funded by EY14259 Genetic Analysis of Retinal Genglion Celll Function, Development and Disease (T.G.).

Disclosure: **J.A. Brzezinski IV**, None; **N.L. Brown**, None; **A. Tanikawa**, None; **R.A. Bush**, None; **P.A. Sieving**, None; **M.H. Vitaterna**, None; **J.S. Takahashi**, None; **T. Glaser**, None

function of the SCN clock. RGCs are not required to generate any of the major ERG waveforms in mice, including the STR, which is produced by ganglion cells in some other species. The diminished amplitude of b-wave, OPs, and STR components in *Math5* mutants is most likely caused by the decreased abundance of retinal interneurons.

The vertebrate retina is an ordered laminar tissue with seven major cell types: rod and cone photoreceptors; horizontal, bipolar, and amacrine interneurons; Müller glia; and retinal ganglion cells (RGCs). These are formed from multipotent retinal progenitors in a stereotyped, temporally overlapping fashion, with RGCs as the first-born cell type in all species examined.[1,2] Retinal progenitor cells express the conserved basic helix-loop-helix (bHLH) transcription factor *ath5*.[3–7] Loss-of-function studies in zebrafish and mice and gain-of-function studies in chicken and frog show that *ath5* is essential for RGC development.[3,4,6–9] Mice with targeted deletions of *Math5* (*Atoh7*) lack RGCs and optic nerves.[8,10] They also have thinner retinas than wild-type mice, with fewer rod bipolar cells, Müller glia and calretinin-positive amacrine cells, but relatively more cones and cholinergic amacrines.[8,10]

In mammals, circadian behavior and physiological rhythms are regulated by an intrinsic pacemaker located in the suprachiasmatic nuclei (SCN) of the hypothalamus.[11,12] Its period approximates 24 hours and is maintained through oscillatory networks of gene expression.[12,13] Under normal circumstances, the SCN clock is synchronized daily to environmental cues, primarily changes in ambient light intensity (photoentrainment).[14] A subset of RGC axons projects directly to the SCN via the retinohypothalamic tract (RHT).[11,15] Eye enucleation and RHT lesion studies in rodents have shown that electrical signals transmitted by RGC axons to the SCN are absolutely necessary for photoentrainment.[16,17] However, neither rod nor cone photoreceptors are required.[18–20] Instead, the RGCs that project directly to the SCN express the photopigment melanopsin (*Opn4*), are intrinsically photosensitive, and mediate photoentrainment.[21–24] However, melanopsin and RGC photosensitivity are not necessary in mice with intact rods and cones.[25,26] Taken together, these observations show RGCs detect light, directly or indirectly, integrate this information, and transmit a signal to the SCN for photoentrainment. However, it remains unclear whether RGCs affect the development and/or intrinsic physiology of the SCN.

Light stimulation triggers a series of changes in electrical potential as the signal is transmitted through the retina from photoreceptors to RGCs and the brain. These electrophysiological changes can be measured using the flash electroretinogram (ERG). For the rod transmission pathway, ERGs are recorded under dark-adapted (scotopic) conditions. The scotopic ERG has four primary components that depend on the intensity of the stimulus flash.[27–31] The scotopic a-wave is a negative waveform generated by hyperpolarization of rods and is detected only at relatively high stimulus intensities.[32,33] The scotopic b-wave is a positive waveform that reflects the depolarization of rod bipolar cells.[31,34–37] The scotopic threshold response (STR) is a sensitive waveform detected at rod threshold light intensities[27–29,38] and is biphasic in rodents.[39,40] The STR is most likely caused by depolarization of amacrine cells and/or RGCs in the rod pathway.[29,30,38,41] Oscillatory potentials (OPs) are regular wavelets that overlay the b-wave and are also thought to arise from depolarizing amacrine cells and/or RGCs.[42–44]

To measure the electrophysiological responses of the cone pathway, flash ERGs are recorded under light-adapted (photopic) conditions. The photopic a-wave, caused by hyperpolarization of cones, is very small in mice because of the small number of cones present and the absence of an anatomic fovea. Depolarization of cone ON bipolar cells generates the photopic b-wave.[45–47]

In this study, we have tested how agenesis of RGCs affects circadian behavior and retinal electrophysiology. We show that *Math5*-null mice cannot photoentrain due to the absence of

RGCs innervating the SCN. In contrast to results in a similar behavioral study in an independent strain of *Math5*-null mice,[48] our mutant mice were free-running with a period that is indistinguishable from that of wild-type littermates, suggesting that the SCN clock is not affected by the congenital absence of RGCs and does not require *Math5* during development. *Math5*-null mice have decreased a- and b-wave, STR, and OP amplitudes, but the shape and time course of ERG components are normal. The number of rod photoreceptors and bipolar cells was reduced in *Math5* mutant mice, commensurate with these ERG changes.

Materials and Methods

Animals

Wild-type and *Math5*-null littermates were derived from one of our original embryonic stem (ES) cell–derived chimeric founders[8] by back-crossing to inbred C57BL/6J mice for four generations and then intercrossing the incipient congenic progeny. The resulting B6.129-*Atoh7*^{tm1Gla} N_4F_2 offspring, which were >90% genetically identical with C57BL/6J, were used for circadian behavioral, RHT labeling, ERG recording, and cell-counting experiments. N_6F_2 mice were used for bipolar and RGC immunohistochemistry experiments. All animals in this study were treated in accordance with the ARVO Statement for the Use of Animals in Ophthalmic and Vision Research.

Circadian Behavioral Testing

At 12 weeks of age, 17 wild-type and 7 *Math5*-null mice were housed individually in cages equipped with running wheels.[14,49] These were assorted randomly into groups of three to four cages and placed inside light-controlled cabinets for 100 days, from November 2000 to February 2001. Wheel-running activity was monitored continuously by an online computer system (Chronobiology Kit; Stanford Software Systems, Santa Cruz, CA) and analyzed in double-plotted actograms. After a 2-day period of adaptation, mice were maintained on a 12-hour light/12-hour dark (LD) cycle for 18 days. The LD cycle was then advanced 6 hours and maintained for 14 days. The mice were then subjected to complete darkness (DD) for 24 days, returned to 12-hour LD for 24 days, and finally exposed to constant light (LL) for 18 days. There was a 5-day gap in activity recording (during the DD phase) when the computer monitoring system failed.

Anterograde Labeling of Retinal Hypothalamic Tracts

The retinal hypothalamic tracts (RHTs) of three wild-type and three *Math5*-null animals were labeled at 8 weeks of age with horseradish peroxidase (HRP)–conjugated cholera toxin B (CT-HRP). Each mouse was deeply anesthetized with 90 mg/kg ketamine and 5 mg/kg xylazine, and 3 μL of 0.2% CT-HRP (List Scientific, Campbell, CA) was slowly injected into one vitreous chamber with a 5-μL syringe with a beveled point (Hamilton, Reno, NV).[50] Mice were given 0.075 mg/kg buprenorphine to minimize discomfort. After 36 hours, mice were euthanatized with an overdose of anesthesia and perfused with 4% paraformaldehyde. To verify the injection and control for nonspecific staining, retinas from injected and uninjected eyes of each mouse were stained for 5 to 10 minutes with 0.5 mg/mL 3,3′-diaminobenzidine tetrahydrochloride (DAB; Sigma-Aldrich, St. Louis, MO) and 0.003% H_2O_2 to reveal HRP activity. The brains were cryoprotected with sucrose, frozen in optimal cutting temperature media (OCT, Tissue Tek; Sakura Finetek, Torrance, CA) and sectioned through the hypothalamus in the coronal plane. To evaluate the RHT, 40-μm cryosections were stained with 0.05 mg/mL 3,3′,5,5′ tetramethylbenzidine (TMB; Sigma-Aldrich) and 0.006% H_2O_2 for 25 minutes.[51] The optic nerves, chiasm and tracts, and SCN were photographed with a compound microscope (Eclipse E800; Nikon, Melville, NY) equipped with Nomarski optics and a digital camera (SPOT; Diagnostic Instruments, Sterling Heights, MI).

Electroretinography

Flash ERGs were recorded from each eye of five wild-type and five *Math5*-null mice at 8 months of age. The mice were dark adapted overnight and anesthetized with 13 mg/kg xylazine and 86 mg/kg ketamine in dim red light. Body temperature was maintained near 38°C with a heating pad. The pupils were dilated with 0.1% atropine and 0.1% phenylephrine HCl, and the corneas were anesthetized with 1% tetracaine. Gold-wire reference electrodes were applied to each cornea under 3% methylcellulose. Gold-wire differential electrodes were placed on the sclera near the limbus, and a ground wire was attached to the ear. Voltage responses were amplified 10,000-fold and passed through 0.1- to 1000-Hz band-pass and 60-Hz notch filters. Full-field 30-μs flashes were generated with a photostrobe (Xenon PS-22; Grass Telefactor, West Warwick, RI) and presented in a Ganzfeld bowl. The stimulus intensity was varied from ERG threshold to a maximum of 0.6 log cd-s/m^2 with neutral-density filters. Photopic ERGs were elicited with 0.6-log cd-s/m^2 maximum intensity flashes on a rod-suppressing white background (42 cd/m^2). S- and M-cone-specific responses were evaluated in wild-type mice with 1-μs photostrobe flashes (model 238; Vivitar USA, Oxnard, CA) that were limited to 400 or 540 nm with narrow-band interference filters (nominal half-bandwidth of 10 nm). To assess relative S-cone versus M-cone responses in *Math5* mutants, we adjusted the strobe intensity to give equal amplitude responses at both wavelengths in wild-type mice.

ERGs were analyzed by plotting the amplitude (in microvolts) of each component against the logarithm of the flash intensity over the entire stimulus range. The a-wave amplitude was measured from pre-stimulus baseline to peak negative voltage, and the b-wave amplitude was measured from the a-wave trough to the b-wave peak. OPs were isolated by subtracting dark-adapted responses recorded at maximum stimulus intensity, with and without 100- to 300-Hz filtering. The amplitudes of OP wavelets 1 to 4 were measured from peak to trough and summed. The implicit time of each ERG component was measured as the time between the flash onset and stimulus peak voltage.

Histology and Morphometric Analysis

After ERG recording, eyes from four wild-type and four mutant animals were fixed in 4% paraformaldehyde, embedded in paraffin, sectioned at 3 μm, and stained with hematoxylin and eosin (H&E) or antibodies. Two central, 250-μm-wide fields were analyzed in midaxial sections of each eye (Fig. 5C). The sections were made near the posterior pole, as close as possible to the longitudinal axis, and were oriented perpendicular to the retinal layers. Laminar thickness was measured at ten 25 μm-spaced intervals and averaged. The planimetric density (cells per square millimeter) of each layer was determined by counting nuclei within the inner (INL) and outer (ONL) nuclear layers in H&E-stained fields, dividing by the section thickness (3 μm) and field width (250 μm), and applying the modified Abercrombie method to correct for nuclear diameter.[52,53]

Rod photoreceptors were counted in adjacent sections. Three wild-type sections (six 250-μm fields) and two *Math5*-null sections (four 250-μm fields) were stained with the rhodopsin monoclonal antibody RetP1[54,55] (1:250; Sigma-Aldrich) and visualized using biotinylated anti-mouse IgG (Jackson ImmunoResearch, West Grove, PA), streptavidin-HRP (ABC; Vector Laboratories, Burlingame, CA), and DAB. All well-defined, rhodopsin-positive perikarya in the ONL of surveyed fields were counted as rods.

Bipolar and RGC Immunofluorescence Staining

Cryosections from wild-type and *Math5*-null mice were immunostained with bipolar and ganglion cell-specific markers.[56] RGCs were labeled with mouse anti-neurofilament 160 kDa (NN18, 1:100; Sigma-Aldrich). Rod bipolar cells were labeled with mouse anti-PKC (MC5, 1:100; Sigma-Aldrich). Cone bipolar cells were stained with mouse anti-$G_o\alpha$ (MAB3073,

1:500; Chemicon, Temecula, CA) and rabbit anti-recoverin (1:1000; the generous gift of Alexander Dizhoor, Kresge Eye Institute, Detroit, MI). Slides were blocked in 10% donkey serum, 1% bovine serum albumin (BSA) in 0.1 M $NaPO_4$ (pH 7.3), 0.5% Triton X-100 (PBTx) for 1.5 to 4 hours at room temperature (RT) and incubated with primary antisera overnight at 4°C. Biotinylated secondary antibodies (1:500; Jackson ImmunoResearch) were added for 2 hours at RT, followed by streptavidin-DTAF (dichlorotriazinylaminofluorescein, 1:500; Jackson ImmunoResearch) for 1 to 2 hours at RT. Images were captured using a confocal fluorescence microscope (Diaphot 200; Nikon) with a laser scanning assembly (Noran OZ; Thermo Electron Corp., Waltham, MA).

Results

Abnormal Circadian Behavior in *Math5*-null Mice

Mammalian circadian clocks are entrained daily to periodic changes in the external environment such as ambient light intensity. The eyes and optic nerves are necessary components of the mammalian photoentrainment pathway. In several species, bilateral eye enucleation or optic nerve transection has been shown to result in circadian behavior that is free-running with an intrinsic period that is slightly longer or shorter than 24 hours.[16,17] Because *Math5*-null mice lack optic nerves at all stages of life, they represent a unique model for testing how congenital absence of RGC input affects SCN development and function.

We measured the circadian wheel-running behavior of 7 $Math5^{-/-}$ and 17 $Math5^{+/+}$ congenic mice, which were age and sex matched. Wheel-running activity was recorded over a 100-day protocol (Fig. 1). During the first 18 days, under 12-hour LD conditions, the wild-type mice exhibited a normal daily activity pattern. They started running shortly after the onset of darkness and stopped running gradually before the onset of light. The correlation between LD and activity cycles indicates that their circadian rhythms were photoentrained. When the LD cycle was advanced 6 hours, the wild-type mice adjusted their rhythms. In contrast, the *Math5*-null mice initiated their activity cycles progressively earlier every day, regardless of the LD stimulus or phase shift in the LD cycle. This free-running behavior indicates that the SCN clock in *Math5*-null mice is not photoentrained.

To test whether the *Math5* mutation alters the intrinsic properties of the SCN clock, activity was recorded in complete darkness (DD) for 24 days (Fig. 1). In the absence of a light signal, both groups of mice had free-running patterns, with an intrinsic period similar to that previously observed for inbred C57BL/6J mice.[57,58] The free-running period length (τ), measured from the onset of activity, was 23.4 ± 0.19 hours (±SD) for $Math5^{+/+}$ and 23.6 ± 0.15 hours for $Math5^{-/-}$ mice. The variance of τ and overall wheel-running activity were also similar in these two groups. When the LD stimulus resumed, the wild-type mice entrained immediately, whereas the *Math5* mutants continued to exhibit free-running behavior. Finally, the mice were subjected to constant light for 18 days (Fig. 1). Under LL conditions, the wild-type mice were free-running with a period greater than 24 hours (24.7 ± 0.59), as expected.[59,60] In contrast, all seven of the *Math5*-null mice continued to free-run with a period <24 hours. Taken together, these data show that development and function of the SCN clock do not depend on *Math5* or RGC innervation.

Absent Retinohypothalamic Tracts in *Math5* Mutants

To verify that the clock-blind phenotype of *Math5*-null mice is due to complete absence of an entrainment signal from the eye, we evaluated the retinohypothalmic tracts (RHTs) by anterograde labeling in vivo. CT-HRP was injected into the vitreous chamber in one eye of three wild-type and three *Math5*-null mice (Fig. 2A). This tracer is readily internalized by

RGCs adjacent to the vitreous and is actively transported along RGC axons to the brain.[61] The uninjected contralateral eye served as a negative control.

Coronal sections through the hypothalamus were stained for peroxidase activity to reveal RHT innervation of the SCN. In wild-type mice, the ipsilateral optic nerve and RHT stained intensely (Fig. 2B). Bilateral staining was observed in the optic chiasm, optic tracts, and SCN. Other RGC projection sites were also labeled, such as the lateral geniculate nuclei and superior colliculi (data not shown). In contrast, *Math5*-null mice showed no staining in the SCN (Fig. 2C, arrow) or other brain regions, but did have HRP activity within the retina of the injected eye (data not shown). Therefore, the circadian behavior of *Math5*-null mice can be explained anatomically by the absence of an RHT.

Electroretinogram Abnormalities in *Math5* Mutants

To evaluate how the lack of RGCs in *Math5* mutant mice alters the electrical physiology of the retina, we compared flash ERG responses. The shape, timing, and amplitude of ERG waveforms are sensitive aggregate measures of retinal function.[62–64] Moreover, the amplitude of ERG a- and b-waves is directly related to the number of cells responding to the light stimulus.[31]

ERGs were recorded from five congenic wild-type and five *Math5*-null mice (Fig. 3). Under dark-adapted conditions, both groups exhibited a biphasic STR (Fig. 3A, arrows) at low light intensity. At higher flash intensities, a- and b-waves were observed, which increased in amplitude according to the stimulus, and OPs became visible (Fig. 3A, arrowheads). Each major waveform was present in the *Math5* mutant ERGs, with a time of onset (latency) similar to wild-type, indicating that the electrophysiology of the rod pathway is grossly normal. However, the *Math5*-null mice had markedly decreased scotopic a- and b-wave amplitudes (Fig. 3A, note difference in scale bars). The b-wave reduction was greater, resulting in a negative overall waveform at the highest stimulus intensities. Under light-adapted (photopic) conditions, which isolate the cone pathway, *Math5*-null mice also had decreased a- and b-wave amplitudes (Fig. 3B). However, because the photopic a-wave is small in rodents and may have contributions from post-synaptic neurons,[65] its amplitude cannot be used reliably to gauge cone photoreceptor abundance at these intensities. There was no change in the spectral sensitivity of the photopic ERG (data not shown), suggesting that the ratio between S- and M-cones is not altered by the *Math5* mutation.

To evaluate the scotopic ERG waveform effects in detail, we overlaid STR, a-wave and b-wave traces recorded from $Math5^{+/+}$ and $Math5^{-/-}$ mice. The shape and timing of the STR was similar for both genotypes, but a 30-fold brighter stimulus was needed for null mice to achieve the same response amplitude as wild-type mice (Fig. 3C). The ERGs recorded at maximum stimulus intensity were averaged within wild-type and null groups, normalized using the average a-wave amplitude of the wild-type mice, and superimposed to compare the timing and relative amplitude of a- and b-waves.[66] The latency and shape of these responses were nearly identical in wild-type and mutant mice (Fig. 3D). However, the b-wave was more severely reduced in amplitude than the a-wave in *Math5* mutants, an effect that is opposite to the ERG changes observed in animal models of photoreceptor degeneration.[66–68]

Quantitative analysis of the ERG data showed that absolute scotopic b-wave amplitudes were significantly lower in *Math5*-null mice than in wild-type mice at all light intensities (Fig. 4A, *t*-test, $P < 0.05$). A 15-fold greater stimulus intensity was needed to achieve a 30-μV scotopic b-wave response in mutant mice than in wild-type mice. Scotopic a-wave amplitudes were also significantly lower in *Math5*-null mice at all intensities above 0.01 cd-s/m^2. Similarly, the photopic b-wave amplitudes were significantly lower in *Math5*-null than in wild-type mice at all intensities (Fig. 4B, *t*-test, $P < 0.05$). Mutants needed four times more light than wild-type

mice to achieve a 30-μV photopic b-wave response. Finally, the mutants had reduced oscillatory wavelet amplitudes in the scotopic ERG. This reduction in the sum of OP amplitudes was greater than the reduction in a- and b-waves (Fig. 4D). There was no difference in the implicit time of any ERG component between wild-type and mutant mice (Fig. 4C). To assess the correlation between scotopic a- and b-wave responses, we plotted amplitudes recorded from individual mutant and wild-type eyes at maximum stimulus intensity.[66] The b- to a-wave ratio was consistently decreased in *Math5* mutants, with a linear regression slope for V_b versus V_a that is one half that of wild-type (Fig. 4E).

Decreased Laminar Thickness and Planimetric Cell Density in Mutant Retinas

The reduced ERG amplitudes in *Math5* mutants suggest alterations in the size and/or connectivity of retinal cell populations. Indeed, differences in the relative abundance of Müller glial, bipolar, cone, and amacrine cells have been noted in *Math5*-null mice.[8,10] It is clear that *Math5* mutant retinas have thinner inner plexiform (IPL), inner nuclear (INL), and outer nuclear (ONL) layers than wild-type mice (Figs. 5A, 5B). To understand the basis of the ERG effects, we compared the cellularity of C57BL/6J congenic wild-type and mutant retinas quantitatively in H&E-stained paraffin-embedded sections. We first measured the radial thickness of the INL, ONL, IPL, and outer plexiform layer (OPL) in two central fields within each retina (Figs. 5C, 5D). We then counted the number of INL and ONL cells in each field and determined their planimetric density (Fig. 5E).

In *Math5* mutants, the IPL was 40% thinner and the INL was 45% thinner than in wild-type (*t*-test, $P < 0.001$). We also observed smaller but statistically significant reductions in the mutant OPL and ONL, which were 12% and 14% thinner than the wild-type, respectively (*t*-test, $P < 0.05$). Planimetric density was calculated for the INL and ONL after correcting the cell counts per field for the section thickness and the nuclear diameter, which was similar in wild-type and *Math5*-null neurons (data not shown). These densities were then normalized to the wild-type values (110,000 and 428,000 nuclei per square millimeter for the INL and ONL, respectively), which were similar to data reported by Jeon et al.[69] for C57BL/6J mice. In the *Math5*-null mice, the INL planimetric density was reduced by 38%, and the ONL planimetric density was reduced by 15% (*t*-test, $P < 0.05$). This decrease is proportional to the reduction in laminar thickness.

Fewer Rods in *Math5* Mutants

The reduction in the number of ONL cells, combined with the diminished scotopic a-wave amplitudes, suggests there are fewer rods in *Math5*-null mice. To measure this directly, we counted rod nuclei in paraffin-embedded sections adjacent to those used for thickness and cell density measurements (Figs. 6A, 6B). Rods were identified using the RetP1 antibody, which labels perikarya in addition to inner and outer segments.[54,55] The *Math5*-null mice had 28% fewer rods than the wild-type mice (*t*-test, $P < 0.001$), similar to the decrease in ONL cells.

Pan-specific Reduction of Bipolar Cells in *Math5* Mutants

In previous studies, we found an equivalent number of amacrine cells in the INL of wild-type and *Math5* mutant mice.[8] The INL thinning and diminished b-wave amplitudes are thus most likely due to a decrease in the number of bipolar cells. To test this hypothesis, we examined wild-type and *Math5*-null retinas by confocal microscopy, with markers specific for bipolar cell subtypes.

Protein kinase C (PKC) is expressed in the somata and axon termini of all rod bipolar cells.[56] Compared with wild-type retinas, the subcellular distribution of PKC protein in *Math5*-null retinas appeared normal with clearly discernible somata, dendrites, axons, and termini (Figs.

7A, 7B). However, the PKC-positive bipolar cells had shorter axons and were ~30% less abundant in the mutants.

The heterotrimeric G protein $G_o\alpha$ functions in ON bipolar pathways and is required to generate the scotopic and photopic b-waves in the ERG.[70] It is expressed more widely than PKC (Figs. 7A, 7C), by cone ON and rod bipolar cells.[56] We detected $G_o\alpha$ in the somata, dendrites, and axons of both bipolar subtypes (Figs. 7C, 7D). The *Math5*-null retinas had normal $G_o\alpha$expression patterns, but ~40% fewer $G_o\alpha$-positive cells than wild-type retinas (Fig. 7D). There was a greater decrease in the number of $G_o\alpha$-positive cells than PKC-positive cells in *Math5* mutants, indicating that both cone ON and rod bipolar subtypes are reduced.

Recoverin is a calcium-binding protein that is expressed at high levels by rod and cone photoreceptors and to a lesser extent by cone bipolar cells.[56,71–73] In the mouse retina, recoverin is made by cone bipolar cells of the OFF subtype.[74] These cells are identified by their immunopositive axon termini in the outer third of the IPL, within the OFF sublamina (Figs. 7E, 7F, arrowheads). The *Math5*-null retinas had normal recoverin staining patterns compared to wild-type retinas, with discernible bipolar cell somata, axons and presynaptic termini (Figs. 7E, 7F). However, the *Math5*-null retinas had ~60% fewer recoverin-positive cone OFF bipolars, with shorter and more compact presynaptic arbors than in wild-type (Fig. 7F, arrowheads). Taken together, our data show that all three bipolar cell subtypes (cone ON, OFF, and rod) were reduced in *Math5* mutant mice.

DISCUSSION

We have examined the effects of *Math5* mutation and RGC agenesis on SCN clock and retinal function. The results demonstrate a severe disruption of circadian photoentrainment and specific alterations in retinal electrophysiology. These effects can be explained by the absence of RGC axons and secondary changes in the size of retinal cell populations, although other, qualitative changes in cell function and synaptic connectivity cannot be completely excluded.

Clock-Blind *Math5* Mutants

In our wheel-running experiments, the *Math5* mutant mice had rhythmic locomotor behavior patterns with a fixed period of 23.6 ± 0.15 hours regardless of lighting conditions. In this respect, they resemble normal mice in constant darkness (DD). Their circadian clock functions normally, but the photoentrainment mechanism does not. By labeling the RHT, we showed that the anatomic connection between the retina and SCN is absent. *Math5*-null mice are thus genetically clock-blind. The SCN receives no tonic or phasic retinal input. Our mice replicate the free-running behavior of *Opn4*$^{-/-}$ *Gnat*$^{-/-}$ *Cnga3*$^{-/-}$ triple mutants and *Opn4*$^{-/-}$ *rd/rd* double mutants, which lack melanopsin and functional photoreceptors but have intact RHTs.[24,26] These mice were reported to have free-running period lengths of 23.3 and 23.5 hours, respectively, in comparable experimental conditions. Together, these findings show that photic information, whether it is directly detected by RGCs or relayed from rods and cones, must be transmitted by RGCs to the SCN for photoentrainment to occur. Moreover, our results demonstrate that congenital absence of the RHT does not affect the development or intrinsic properties of the SCN, including its innate period length.[75,76]

Recently, an independent *Math5*-null strain was also shown by Wee et al.[48] to be incapable of photoentrainment. In contrast to our strain, these null mice retain a small number of RGCs, approximately 5% to 10% of wild-type, including melanopsin-positive RGCs,[9,48] and were examined on a variably mixed 129SvEv × C57BL/6 genetic background.[10] They exhibited free-running behavior under LD and DD conditions, but had an intrinsic period of 24.4 ± 0.10 hours,[48] similar to normal mice in LL conditions or diurnal mammals in DD conditions. This discrepancy can be explained if the intrinsic circadian machinery in the *Math5* mutants studied

by Wee et al.[48] were functionally altered or if the residual RGCs in these mice transmitted weak, unbalanced, or inappropriate signals to the SCN, either directly or via accessory pathways, such as the intergeniculate leaflet (IGL), resulting in a lengthening of the free-running period. The geniculohypothalamic tract (GHT) has been shown to modulate period length under LL and DD conditions, in conjunction with the RHT.[77–79] The *Math5* mutants studied by Wee et al.[48] have some retinal fibers projecting to the optic chiasm and a very small but measurable pupillary light response.[80] The free-running period length (τ) may depend on the extent of residual RGCs and/or a genetic interaction between the *Math5* mutation and modifiers in the C57BL/6 versus 129SvEv strain background, potentially including loci such as *Cry1*, which is linked to *Math5* (*Atoh7*) on chromosome 10 and is known to control τ.[81–83] Indeed, several quantitative trait loci (QTLs) have been shown to determine τ in crosses between C57BL/6 and other inbred strains.[57–59,84–86] This source of variation was significantly reduced in the C57BL/6J N_4F_2 mice that we examined. Moreover, mice of the eyeless ZRDCT-AN strain also tend to have free-running periods that are >24 hours.[87] These mice have absent or greatly attenuated RHTs and variably abnormal hypothalamic anatomy[88] but intact GHTs,[89] resulting from a point mutation in the *Rx* homeobox gene.[90]

Diminished ERG Responses in *Math5* Mutants

Math5-null mice have b-waves, a-waves, STRs, and OPs that are similar to wild-type in their shape and time course. However, the amplitudes of these waveforms are diminished to a different extent, depending on the retinal layer of origin. The scotopic a-wave, which is generated by photoreceptors,[31] is least affected in the *Math5*-null mice, whereas the scotopic b-wave, STR, and OPs which are generated by interneurons, are significantly reduced. Among these, the STR and OPs are diminished to a greater extent than the b-wave. An opposite pattern is observed in photoreceptor degeneration, which affects the a-wave more than the b-wave, followed by the STR.[66–68] In this situation, electrical potentials generated by second- and third-order neurons postsynaptic to the photoreceptors may decline more slowly because of the large degree of signal convergence and amplification between the outer and inner retina. Other factors may also contribute, such as alterations in the function of remaining neurons[91,92] or reactive changes in Müller glia, which are essential for the STR.[93]

The scotopic b-wave is decreased in *Math5* mutants for two reasons. First, there are fewer rods to detect light and stimulate bipolar cells, and these rods may have a reduced quantal catch. This causes a 58% ± 4% decrease in the scotopic a-wave amplitude (Fig. 4D) and should, by itself, produce a 36% decline in b-wave amplitude. This prediction is based on the linear relationship between a- and b-wave amplitudes in transgenic rhodopsin P23H rats, which have pure rod photoreceptor degeneration.[66] Second, there are ~50% fewer bipolar cells in the *Math5* mutants. Because these cells are primary generators of the b-wave, this should decrease the b-wave amplitude directly. Multiplying these effects, the scotopic b-wave in *Math5* mutants is predicted to be: (1–0.36) × (1–0.5) × 100 = 32% of wild-type, which is close to the observed result (31%, Fig. 4D). Moreover, the slope of the b- versus a-wave amplitude plot is approximately halved in *Math5*-null mice (Fig. 4E). This observation is consistent with the twofold decrease in the number of bipolar cells, assuming that the remaining cells synapse with photoreceptors and function normally.

In *Math5*-null mice, agenesis of ganglion cells and reduction of certain amacrine cell types[8] does not eliminate the STR. Similarly, optic nerve transection with subsequent loss of ganglion cells does not eliminate the negative STR in cats[41] or rats.[40] However, in the macaque monkey, experimental glaucoma causes RGC loss and abolishes the STR.[38] These observations suggest that the relative contribution of amacrine and ganglion cells to the STR differs between species.[39] In our experiments a ~30-fold brighter stimulus was needed to obtain an equivalent amplitude STR response in *Math5* mutants compared with wild-type mice. This effect is larger

than the change in STR produced by optic nerve transection.[41,40] The difference may reflect a concomitant change in amacrine cells in *Math5* mutants or a greater dependence of the STR on ganglion cell activity in mice compared with other species. Previously, we found a reduction in the abundance of calretinin-positive and A2 amacrine cells in *Math5*-null mice.[8] Because A2 cells are the first amacrine cell type in the pathway between rod bipolar and ganglion cells,[94] it is reasonable to expect that their loss could affect the STR.

In our previous study,[8] we found an increase in the relative abundance of cone photoreceptors in *Math5*-null mice, but did not appreciate the decreased rod density and ONL thickness. The absolute number of cones is also increased in *Math5* mutants, but these cells are relatively disorganized compared to the orderly arrangement of cones in wild-type mice. The ~75% reduction in the photopic b-wave (Fig. 4B) can be explained by the ~40% reduction in $G_o\alpha$ bipolar cells (Fig. 7D), particularly if the cone quantal catch and the connectivity between cones and ON bipolar cells were impaired. In the *Nrl* knockout mouse, photopic a- and b-waves are increased dramatically, but not in proportion to the huge increase in cones.[95]

Alterations in Retinal Cell Populations

The ERG data indicate that the number of rod photoreceptors, and rod and cone bipolar cells was reduced in *Math5*-null mice. Quantitative analyses of retinal laminar thickness, planimetric cell density, and rhodopsin staining support these observations. In several respects, the decreased b- and a-wave amplitudes and correlated reduction in INL and ONL cell densities in *Math5* mutants are reminiscent of ERG and histologic changes in *Krd*/+ mice, which have severe malformations of the optic stalk and nerve due to a *Pax2* gene deletion, resulting in a deficiency of RGCs and a six-fold decrease in ganglion cell layer (GCL) density.[52,96] Diminished b-wave amplitudes have also been noted in humans with optic nerve hypoplasia and correlate with disease severity (van Boemel GB, et al. *IOVS* 2002;43:ARVO E-Abstract 909).[97]

All three major classes of bipolar cells (rod, cone ON, cone OFF) are reduced in *Math5*-null mice. The decrease in rod bipolars (PKC- and $G_o\alpha$-positive) can largely explain the reduction in the scotopic b-wave amplitude. The decrease in cone ON bipolars ($G_o\alpha$-positive, PKC-negative) causes the reduction in the photopic b-wave. Because b-waves are present, rod bipolar and cone ON bipolar pathways are clearly functional in *Math5*-null mice. Furthermore, the patterns of PKC, recoverin, and $G_o\alpha$ staining are morphologically normal. These data suggest that the *Math5* mutation changes the abundance of bipolar cells, but does not significantly alter their properties.

Despite the absence of RGCs and secondary alterations in the size of other cell populations, the intraretinal circuitry is generally intact in *Math5* mutants. Moreover, the bipolar cell axons in these mice project to the proper sublaminae in the IPL (Fig. 6, and data not shown). This result is particularly striking since bipolar cells develop after RGCs and synapse on them. Similar results have been observed in rats after early optic nerve transection[98] and in the *ath5* mutant (*lakritz*) zebrafish.[99] Taken together, our findings show that fundamental aspects of retinal wiring do not depend on cues provided by postsynaptic cells or on a functional connection between the eyes and brain.

Acknowledgements

The authors thank Sara Schulz, Sue Tarlé, Emily Wroblewski, Debbie Fenner, Alan Mears, Bruce Donohoe, Steve Lentz, Mitch Gillett, Peter Hitchcock, and Nancy Smith for technical assistance and advice.

References

1. Altschuler, DM.; Turner, DL.; Cepko, CL. Specification of cell type in the vertebrate retina. In: Lam, DMK.; Shatz, CJ., editors. Cell Lineage and Cell Fate in Visual System Development. Cambridge, MA: MIT Press; 1991. p. 37-58.
2. Cepko CL, Austin CP, Yang X, Alexiades M, Ezzeddine D. Cell fate determination in the vertebrate retina. Proc Natl Acad Sci USA 1996;93:589–595. [PubMed: 8570600]
3. Matter-Sadzinski L, Matter JM, Ong MT, Hernandez J, Ballivet M. Specification of neurotransmitter receptor identity in developing retina: the chick ATH5 promoter integrates the positive and negative effects of several bHLH proteins. Development 2001;128:217–231. [PubMed: 11124117]
4. Liu W, Mo Z, Xiang M. The Ath5 proneural genes function upstream of Brn3 POU domain transcription factor genes to promote retinal ganglion cell development. Proc Natl Acad Sci USA 2001;98:1649–1654. [PubMed: 11172005]
5. Brown NL, Kanekar S, Vetter ML, Tucker PK, Gemza DL, Glaser T. Math5 encodes a murine basic helix-loop-helix transcription factor expressed during early stages of retinal neurogenesis. Development 1998;125:4821–4833. [PubMed: 9806930]
6. Kanekar S, Perron M, Dorsky R, et al. Xath5 participates in a network of bHLH genes in the developing Xenopus retina. Neuron 1997;19:981–994. [PubMed: 9390513]
7. Kay JN, Finger-Baier KC, Roeser T, Staub W, Baier H. Retinal ganglion cell genesis requires lakritz, a Zebrafish atonal homolog. Neuron 2001;30:725–736. [PubMed: 11430806]
8. Brown NL, Patel S, Brzezinski J, Glaser T. Math5 is required for retinal ganglion cell and optic nerve formation. Development 2001;128:2497–2508. [PubMed: 11493566]
9. Lin B, Wang SW, Masland RH. Retinal ganglion cell type, size, and spacing can be specified independent of homotypic dendritic contacts. Neuron 2004;43:475–485. [PubMed: 15312647]
10. Wang SW, Kim BS, Ding K, et al. Requirement for math5 in the development of retinal ganglion cells. Genes Dev 2001;15:24–29. [PubMed: 11156601]
11. Klein, DC.; Moore, RY.; Reppert, SM. Suprachiasmatic Nucleus: the Mind's Clock. New York: Oxford University Press; 1991.
12. Lowrey PL, Takahashi JS. Genetics of the mammalian circadian system: photic entrainment, circadian pacemaker mechanisms, and posttranslational regulation. Annu Rev Genet 2000;34:533–562. [PubMed: 11092838]
13. Albrecht U. Invited review: regulation of mammalian circadian clock genes. J Appl Physiol 2002;92:1348–1355. [PubMed: 11842077]
14. Daan, S.; Aschoff, J. The entrainment of circadian systems. In: Takahashi, JS.; Turek, FW.; Moore, RY., editors. Circadian Clocks. Handbooks of Behavioral Neurobiology. Vol. 12. New York: Kluwer Academic Plenum Publishers; 2001. p. 7-43.
15. Provencio I, Cooper HM, Foster RG. Retinal projections in mice with inherited retinal degeneration: implications for circadian photoentrainment. J Comp Neurol 1998;395:417–439. [PubMed: 9619497]
16. Nelson RJ, Zucker I. Absence of extraocular photoreception in diurnal and nocturnal rodents exposed to direct sunlight. Comp Biochem Physiol [A] 1981;69:145–148.
17. Johnson RF, Moore RY, Morin LP. Loss of entrainment and anatomical plasticity after lesions of the hamster retinohypothalamic tract. Brain Res 1988;460:297–313. [PubMed: 2465060]
18. Foster RG, Provencio I, Hudson D, Fiske S, De Grip W, Menaker M. Circadian photoreception in the retinally degenerate mouse (rd/rd). J Comp Physiol [A] 1991;169:39–50.
19. Freedman MS, Lucas RJ, Soni B, et al. Regulation of mammalian circadian behavior by non-rod, non-cone, ocular photoreceptors. Science 1999;284:502–504. [PubMed: 10205061]
20. McCall MA, Gregg RG, Merriman K, Goto Y, Peachey NS, Stanford LR. Morphological and physiological consequences of the selective elimination of rod photoreceptors in transgenic mice. Exp Eye Res 1996;63:35–50. [PubMed: 8983962]
21. Provencio I, Rodriguez IR, Jiang G, Hayes WP, Moreira EF, Rollag MD. A novel human opsin in the inner retina. J Neurosci 2000;20:600–605. [PubMed: 10632589]
22. von Schantz M, Provencio I, Foster RG. Recent developments in circadian photoreception: more than meets the eye. Invest Ophthalmol Vis Sci 2000;41:1605–1607. [PubMed: 10845575]

23. Berson DM, Dunn FA, Takao M. Phototransduction by retinal ganglion cells that set the circadian clock. Science 2002;295:1070–1073. [PubMed: 11834835]
24. Hattar S, Liao HW, Takao M, Berson DM, Yau KW. Melanopsin-containing retinal ganglion cells: architecture, projections, and intrinsic photosensitivity. Science 2002;295:1065–1070. [PubMed: 11834834]
25. Hattar S, Lucas RJ, Mrosovsky N, et al. Melanopsin and rod-cone photoreceptive systems account for all major accessory visual functions in mice. Nature 2003;424:76–81. [PubMed: 12808468]
26. Panda S, Sato TK, Castrucci AM, et al. Melanopsin (Opn4) requirement for normal light-induced circadian phase shifting. Science 2002;298:2213–2216. [PubMed: 12481141]
27. Sieving PA, Frishman LJ, Steinberg RH. Scotopic threshold response of proximal retina in cat. J Neurophysiol 1986;56:1049–1061. [PubMed: 3783228]
28. Sieving PA, Nino C. Scotopic threshold response (STR) of the human electroretinogram. Invest Ophthalmol Vis Sci 1988;29:1608–1614. [PubMed: 3182195]
29. Naarendorp F, Sieving PA. The scotopic threshold response of the cat ERG is suppressed selectively by GABA and glycine. Vision Res 1991;31:1–15. [PubMed: 2006543]
30. Frishman LJ, Sieving PA, Steinberg RH. Contributions to the electroretinogram of currents originating in proximal retina. Vis Neurosci 1988;1:307–315. [PubMed: 3154802]
31. Pugh, EN., Jr; Falsini, B.; Lyubarsky, AL. The origin of the major rod-and cone-driven components of the rodent electroretinogram and the effect of age and light-rearing history on the magnitude of these components. In: Williams, TP.; Thistle, AB., editors. Photostasis and Related Phenomena. New York: Plenum Press; 1998. p. 93-128.
32. Brown KT, Watanabe K, Murakami M. The early and late receptor potentials of monkey cones and rods. Cold Spring Harb Symp Quant Biol 1965;30:457–482. [PubMed: 4956619]
33. Penn RD, Hagins WA. Signal transmission along retinal rods and the origin of the electroretinographic a-wave. Nature 1969;223:201–204. [PubMed: 4307228]
34. Xu X, Karwoski CJ. Current source density analysis of retinal field potentials. II. Pharmacological analysis of the b-wave and M-wave. J Neurophysiol 1994;72:96–105. [PubMed: 7965036]
35. Robson JG, Frishman LJ. Response linearity and kinetics of the cat retina: the bipolar cell component of the dark-adapted electroretinogram. Vis Neurosci 1995;12:837–850. [PubMed: 8924408]
36. Green DG, Kapousta-Bruneau NV. A dissection of the electroretinogram from the isolated rat retina with microelectrodes and drugs. Vis Neurosci 1999;16:727–741. [PubMed: 10431921]
37. Kofuji P, Ceelen P, Zahs KR, Surbeck LW, Lester HA, Newman EA. Genetic inactivation of an inwardly rectifying potassium channel (Kir4.1 subunit) in mice: phenotypic impact in retina. J Neurosci 2000;20:5733–5740. [PubMed: 10908613]
38. Frishman LJ, Shen FF, Du L, et al. The scotopic electroretinogram of macaque after retinal ganglion cell loss from experimental glaucoma. Invest Ophthalmol Vis Sci 1996;37:125–141. [PubMed: 8550316]
39. Saszik SM, Robson JG, Frishman LJ. The scotopic threshold response of the dark-adapted electroretinogram of the mouse. J Physiol 2002;543:899–916. [PubMed: 12231647]
40. Bui BV, Fortune B. Ganglion cell contributions to the rat full-field electroretinogram. J Physiol 2004;555:153–173. [PubMed: 14578484]
41. Sieving PA. Retinal ganglion cell loss does not abolish the scotopic threshold response (STR). Clin Vision Sci 1991;6:149–158.
42. Wachtmeister L. Oscillatory potentials in the retina: what do they reveal. Prog Retin Eye Res 1998;17:485–521. [PubMed: 9777648]
43. Vaegan Graham SL, Goldberg I, Millar TJ. Selective reduction of oscillatory potentials and pattern electroretinograms after retinal ganglion cell damage by disease in humans or by kainic acid toxicity in cats. Doc Ophthalmol 1991;77:237–253. [PubMed: 1760972]
44. Karwoski, C.; Kawasaki, K. Oscillatory potentials. In: Heckenlively, JR.; Arden, GB., editors. Principles and Practice of Clinical Electrophysiology of Vision. St. Louis: Mosby Year Book; 1991. p. 125-128.

45. Nawy S, Sie A, Copenhagen DR. The glutamate analog 2-amino-4-phosphonobutyrate antagonizes synaptic transmission from cones to horizontal cells in the goldfish retina. Proc Natl Acad Sci USA 1989;86:1726–1730. [PubMed: 2537984]
46. Slaughter MM, Miller RF. An excitatory amino acid antagonist blocks cone input to sign-conserving second-order retinal neurons. Science 1983;219:1230–1232. [PubMed: 6131536]
47. Sieving PA, Murayama K, Naarendorp F. Push-pull model of the primate photopic electroretinogram: a role for hyperpolarizing neurons in shaping the b-wave. Vis Neurosci 1994;11:519–532. [PubMed: 8038126]
48. Wee R, Castrucci AM, Provencio I, Gan L, Van Gelder RN. Loss of photic entrainment and altered free-running circadian rhythms in math5−/− mice. J Neurosci 2002;22:10427–10433. [PubMed: 12451142]
49. Low-Zeddies SS, Takahashi JS. Chimera analysis of the clock mutation in mice shows that complex cellular integration determines circadian behavior. Cell 2001;105:25–42. [PubMed: 11301000]
50. Zhang Y, Brainard GC, Zee PC, Pinto LH, Takahashi JS, Turek FW. Effects of aging on lens transmittance and retinal input to the suprachiasmatic nucleus in golden hamsters. Neurosci Lett 1998;258:167–170. [PubMed: 9885957]
51. Mesulam MM. Tetramethyl benzidine for horseradish peroxidase neurohistochemistry: a non-carcinogenic blue reaction product with superior sensitivity for visualizing neural afferents and efferents. J Histochem Cytochem 1978;26:106–117. [PubMed: 24068]
52. Green DG, Kapousta-Bruneau NV, Hitchcock PF, Keller SA. Electrophysiology and density of retinal neurons in mice with a mutation that includes the Pax2 locus. Invest Ophthalmol Vis Sci 1997;38:919–929. [PubMed: 9112988]
53. Nauta, WJH.; Ebbesson, SOE. Contemporary Research Methods in Neuroanatomy. viii. New York: Springer-Verlag; 1970. p. 386
54. Fekete DM, Barnstable CJ. The subcellular localization of rat photoreceptor-specific antigens. J Neurocytol 1983;12:785–803. [PubMed: 6358424]
55. Hicks D, Barnstable CJ. Lectin and antibody labelling of developing rat photoreceptor cells: an electron microscope immunocytochemical study. J Neurocytol 1986;15:219–230. [PubMed: 3755163]
56. Haverkamp S, Wassle H. Immunocytochemical analysis of the mouse retina. J Comp Neurol 2000;424:1–23. [PubMed: 10888735]
57. Ebihara S, Tsuji K, Kondo K. Strain differences of the mouse's free-running circadian rhythm in continuous darkness. Physiol Behav 1978;20:795–799. [PubMed: 684115]
58. Schwartz WJ, Zimmerman P. Circadian timekeeping in BALB/c and C57BL/6 inbred mouse strains. J Neurosci 1990;10:3685–3694. [PubMed: 2230953]
59. Hofstetter JR, Mayeda AR, Possidente B, Nurnberger JI Jr. Quantitative trait loci (QTL) for circadian rhythms of locomotor activity in mice. Behav Genet 1995;25:545–556. [PubMed: 8540893]
60. Possidente B, Hegmann JP. Gene differences modify Aschoff's rule in mice. Physiol Behav 1982;28:199–200. [PubMed: 7200614]
61. Mikkelsen JD. Visualization of efferent retinal projections by immunohistochemical identification of cholera toxin subunit B. Brain Res Bull 1992;28:619–623. [PubMed: 1617444]
62. Newman, EA.; Frishman, LJ. Heckenlively, JR.; Arden, GB. Principles and Practice of Clinical Electrophysiology of Vision. St. Louis: Mosby Year Book; 1991. The b-wave; p. 101-111.
63. Heckenlively JR, Rodriguez JA, Daiger SP. Autosomal dominant sectoral retinitis pigmentosa: two families with transversion mutation in codon 23 of rhodopsin. Arch Ophthalmol 1991;109:84–91. [PubMed: 1987955]
64. Hood DC, Birch DG. Rod phototransduction in retinitis pigmentosa: estimation and interpretation of parameters derived from the rod a-wave. Invest Ophthalmol Vis Sci 1994;35:2948–2961. [PubMed: 8206712]
65. Xu L, Ball SL, Alexander KR, Peachey NS. Pharmacological analysis of the rat cone electroretinogram. Vis Neurosci 2003;20:297–306. [PubMed: 14570251]
66. Machida S, Kondo M, Jamison JA, et al. P23H rhodopsin transgenic rat: correlation of retinal function with histopathology. Invest Ophthalmol Vis Sci 2000;41:3200–3209. [PubMed: 10967084]

67. Bush RA, Hawks KW, Sieving PA. Preservation of inner retinal responses in the aged Royal College of Surgeons rat: evidence against glutamate excitotoxicity in photoreceptor degeneration. Invest Ophthalmol Vis Sci 1995;36:2054–2062. [PubMed: 7657544]
68. Aleman TS, LaVail MM, Montemayor R, et al. Augmented rod bipolar cell function in partial receptor loss: an ERG study in P23H rhodopsin transgenic and aging normal rats. Vision Res 2001;41:2779–2797. [PubMed: 11587727]
69. Jeon CJ, Strettoi E, Masland RH. The major cell populations of the mouse retina. J Neurosci 1998;18:8936–8946. [PubMed: 9786999]
70. Dhingra A, Jiang M, Wang TL, et al. Light response of retinal ON bipolar cells requires a specific splice variant of Galpha(o). J Neurosci 2002;22:4878–4884. [PubMed: 12077185]
71. Milam AH, Dacey DM, Dizhoor AM. Recoverin immunoreactivity in mammalian cone bipolar cells. Vis Neurosci 1993;10:1–12. [PubMed: 8424920]
72. Euler T, Wassle H. Immunocytochemical identification of cone bipolar cells in the rat retina. J Comp Neurol 1995;361:461–478. [PubMed: 8550893]
73. Dizhoor AM, Ray S, Kumar S, et al. Recoverin: a calcium sensitive activator of retinal rod guanylate cyclase. Science 1991;251:915–918. [PubMed: 1672047]
74. Haverkamp S, Ghosh KK, Hirano AA, Wassle H. Immunocytochemical description of five bipolar cell types of the mouse retina. J Comp Neurol 2003;455:463–476. [PubMed: 12508320]
75. Yamazaki S, Alones V, Menaker M. Interaction of the retina with suprachiasmatic pacemakers in the control of circadian behavior. J Biol Rhythms 2002;17:315–329. [PubMed: 12164248]
76. Pittendrigh CS, Daan S. A functional analysis of circadian pacemakers in nocturnal rodents, I: the stability and lability of spontaneous frequency. J Comp Physiol [A] 1976;106:223–252.
77. Pickard GE. Intergeniculate leaflet ablation alters circadian rhythms in the mouse. Neuroreport 1994;5:2186–2188. [PubMed: 7865773]
78. Pickard GE, Ralph MR, Menaker M. The intergeniculate leaflet partially mediates effects of light on circadian rhythms. J Biol Rhythms 1987;2:35–56. [PubMed: 2979650]
79. Morin LP, Pace L. The intergeniculate leaflet, but not the visual midbrain, mediates hamster circadian rhythm response to constant light. J Biol Rhythms 2002;17:217–226. [PubMed: 12054193]
80. Van Gelder RN, Wee R, Lee JA, Tu DC. Reduced pupillary light responses in mice lacking cryptochromes. Science 2003;299:222. [PubMed: 12522242]
81. Vitaterna MH, Selby CP, Todo T, et al. Differential regulation of mammalian period genes and circadian rhythmicity by cryptochromes 1 and 2. Proc Natl Acad Sci USA 1999;96:12114–12119. [PubMed: 10518585]
82. van der Horst GT, Muijtjens M, Kobayashi K, et al. Mammalian Cry1 and Cry2 are essential for maintenance of circadian rhythms. Nature 1999;398:627–630. [PubMed: 10217146]
83. Thresher RJ, Vitaterna MH, Miyamoto Y, et al. Role of mouse cryptochrome blue-light photoreceptor in circadian photoresponses. Science 1998;282:1490–1494. [PubMed: 9822380]
84. Shimomura K, Low-Zeddies SS, King DP, et al. Genome-wide epistatic interaction analysis reveals complex genetic determinants of circadian behavior in mice. Genome Res 2001;11:959–980. [PubMed: 11381025]
85. Suzuki T, Ishikawa A, Yoshimura T, et al. Quantitative trait locus analysis of abnormal circadian period in CS mice. Mamm Genome 2001;12:272–277. [PubMed: 11309657]
86. Hofstetter JR, Mayeda AR. Provisional quantitative trait loci (QTL) for the Aschoff effect in RI mice. Physiol Behav 1998;64:97–101. [PubMed: 9661988]
87. Laemle LK, Ottenweller JE. Daily patterns of running wheel activity in male anophthalmic mice. Physiol Behav 1998;64:165–171. [PubMed: 9662081]
88. Silver J. Abnormal development of the suprachiasmatic nuclei of the hypothalamus in a strain of genetically anophthalmic mice. J Comp Neurol 1977;176:589–606. [PubMed: 925203]
89. Laemle LK, Fugaro C, Bentley T. The geniculohypothalamic pathway in a congenitally anophthalmic mouse. Brain Res 1993;618:352–357. [PubMed: 8374768]
90. Tucker P, Laemle L, Munson A, et al. The eyeless mouse mutation (ey1) removes an alternative start codon from the Rx/rax homeobox gene. Genesis 2001;31:43–53. [PubMed: 11668677]

91. Cuenca N, Pinilla I, Sauve Y, Lu B, Wang S, Lund RD. Regressive and reactive changes in the connectivity patterns of rod and cone pathways of P23H transgenic rat retina. Neuroscience 2004;127:301–317. [PubMed: 15262321]
92. Du JL, Poo MM. Rapid BDNF-induced retrograde synaptic modification in a developing retinotectal system. Nature 2004;429:878–883. [PubMed: 15215865]
93. Frishman LJ, Steinberg RH. Light-evoked increases in [K+]o in proximal portion of the dark-adapted cat retina. J Neurophysiol 1989;61:1233–1243. [PubMed: 2746323]
94. Sharpe LT, Stockman A. Rod pathways: the importance of seeing nothing. Trends Neurosci 1999;22:497–504. [PubMed: 10529817]
95. Mears AJ, Kondo M, Swain PK, et al. Nrl is required for rod photoreceptor development. Nat Genet 2001;29:447–452. [PubMed: 11694879]
96. Otteson DC, Shelden E, Jones JM, Kameoka J, Hitchcock PF. Pax2 expression and retinal morphogenesis in the normal and Krd mouse. Dev Biol 1998;193:209–224. [PubMed: 9473325]
97. Janaky M, Deak A, Pelle Z, Benedek G. Electrophysiologic alterations in patients with optic nerve hypoplasia. Doc Ophthalmol 1994;86:247–257. [PubMed: 7813376]
98. Gunhan-Agar E, Kahn D, Chalupa LM. Segregation of on and off bipolar cell axonal arbors in the absence of retinal ganglion cells. J Neurosci 2000;20:306–314. [PubMed: 10627608]
99. Kay JN, Roeser T, Mumm JS, et al. Transient requirement for ganglion cells during assembly of retinal synaptic layers. Development 2004;131:1331–1342. [PubMed: 14973290]

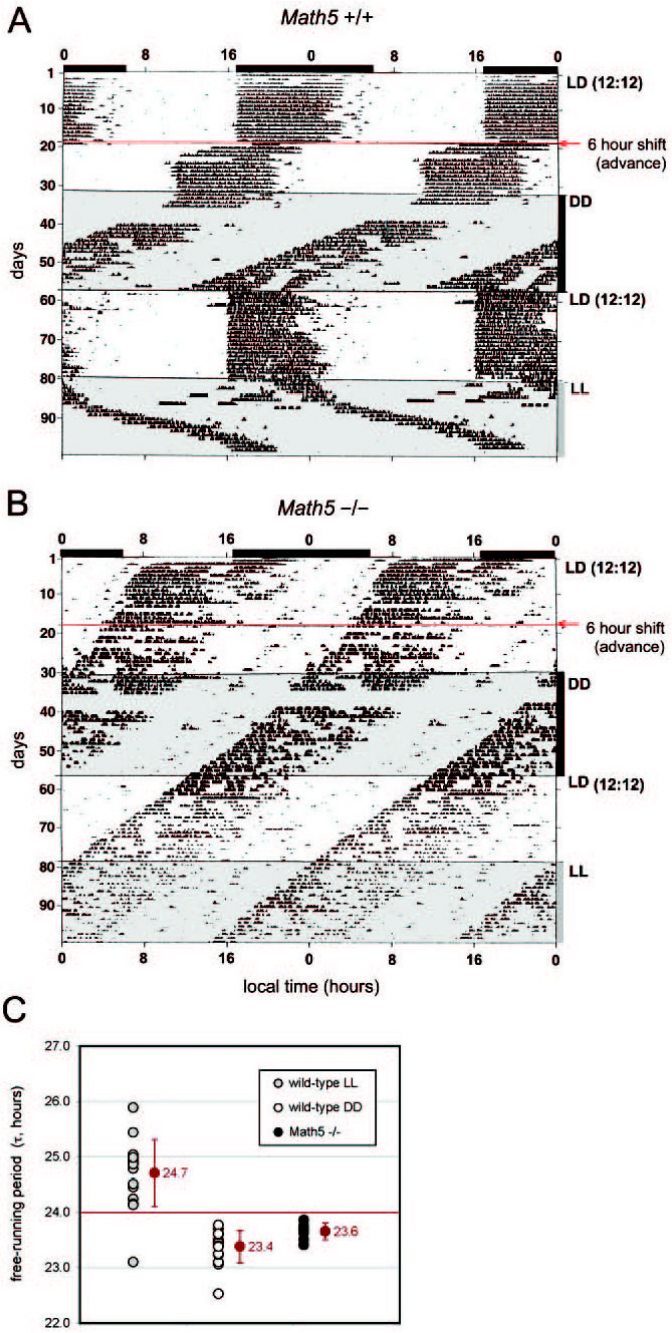

Figure 1.

Math5-null mice exhibit free-running circadian behavior. Actograms show wheel-running behavior for representative *Math5*$^{+/+}$ (**A**) and *Math5*$^{-/-}$ (**B**) mice. Local clock time is double-plotted across the horizontal axis with the light stimulus indicated. The amplitude of the tick marks shows the intensity of wheel-running activity. The data were recorded during a single 100-day experiment, as indicated on the vertical axis. (**A**) Wild-type mice had wheel-running patterns that started and finished at the same clock time each day under LD conditions and were therefore photoentrained. When the LD cycle was advanced 6 hours, wild-type mice entrained to the new cycle within a few days, advancing their behavior by 6 hours. In constant darkness (DD), the wild-type mice were free-running with a 23.4-hour period (n = 17). On

returning to LD, the mice were re-entrained, with a 24-hour period. In LL, the mice were free-running with a 24.7-hour period ($n = 17$). (**B**) *Math5*$^{-/-}$ mice were free-running under all light conditions, with a 23.6-hour period ($n = 7$). They resembled wild-type mice in DD. Their SCN clocks were intrinsically normal but did not photoentrain. (**C**) Free-running periods for each animal under DD and LL conditions, with the group averages ± SD (*red*). LD, 12 hours light-dark.

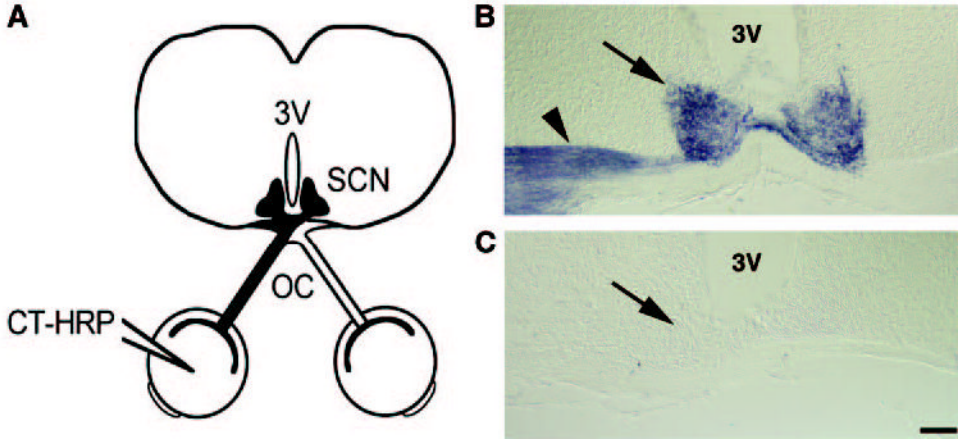

Figure 2.

Math5-null mice lack retinohypothalamic tracts. (**A**) CT-HRP was injected into one eye, labeling its optic nerve and projections in the brain, including the optic chiasm (OC) and suprachiasmatic nuclei (SCN). Coronal brain sections were stained with TMB to visualize RGC projections. (**B**) In wild-type mice, the ipsilateral RHT (*arrowhead*) and both SCN (*arrow*) were labeled, whereas the contralateral RHT was unstained. (**C**) In *Math5*$^{-/-}$ mice, the SCN (*arrow*) and the RHT were unstained. The ventral surface is at the *bottom* of each panel. 3V, third ventricle. Scale bar, 100 μm.

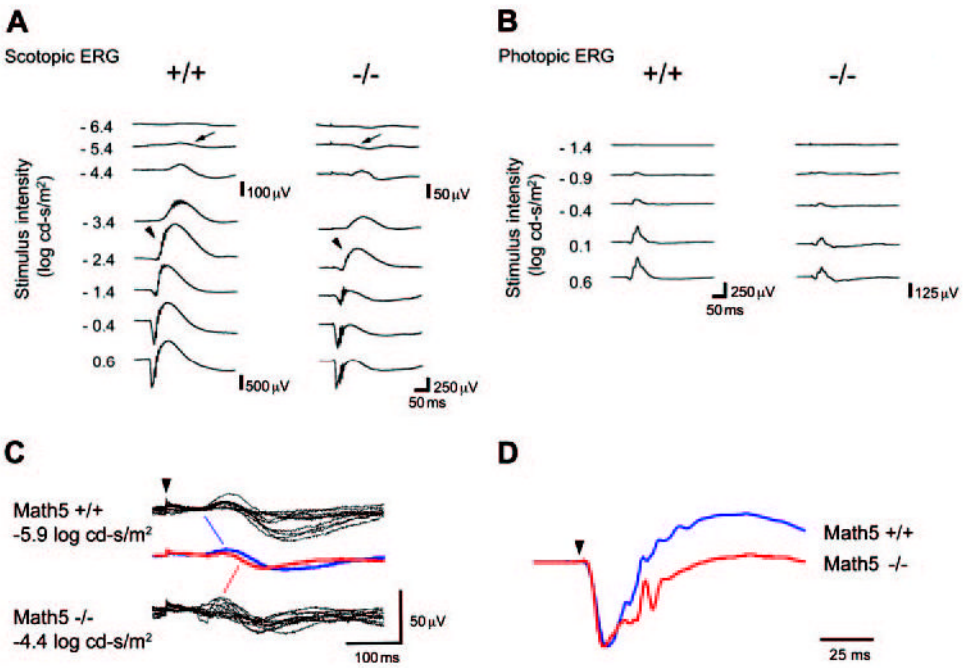

Figure 3.

Math5-null mice have diminished flash ERGs. (**A**) Representative scotopic ERG recordings. *Math5*$^{-/-}$ mice have decreased a- and b-wave amplitudes (note the difference in scale bars). The STR (*arrows*) and OPs (*arrowheads*) are indicated. (**B**) Photopic ERG recordings. *Math5*$^{-/-}$ mice have decreased b-wave amplitudes (note the difference in scale bars). (**C**) STRs recorded from 10 wild-type (*top*) and 10 *Math5*$^{-/-}$ (*bottom*) eyes. Waveforms were elicited by a −5.9 and −4.4 log cd-s/m^2 light stimulus. Averaged responses for wild-type (*blue*) and *Math5*$^{-/-}$ (*red*) mice are superimposed in the center. *Math5* mutants required a 30-fold greater stimulus intensity to generate an STR comparable to wild-type mice. (**D**) Scotopic ERGs averaged from 10 wild-type and 10 *Math5*$^{-/-}$ eyes at the maximum stimulus (0.6 log cd-s/m^2) are normalized and superimposed to compare the timing and relative amplitude of a- and b-waves. The b-wave amplitude is decreased more than the a-wave.

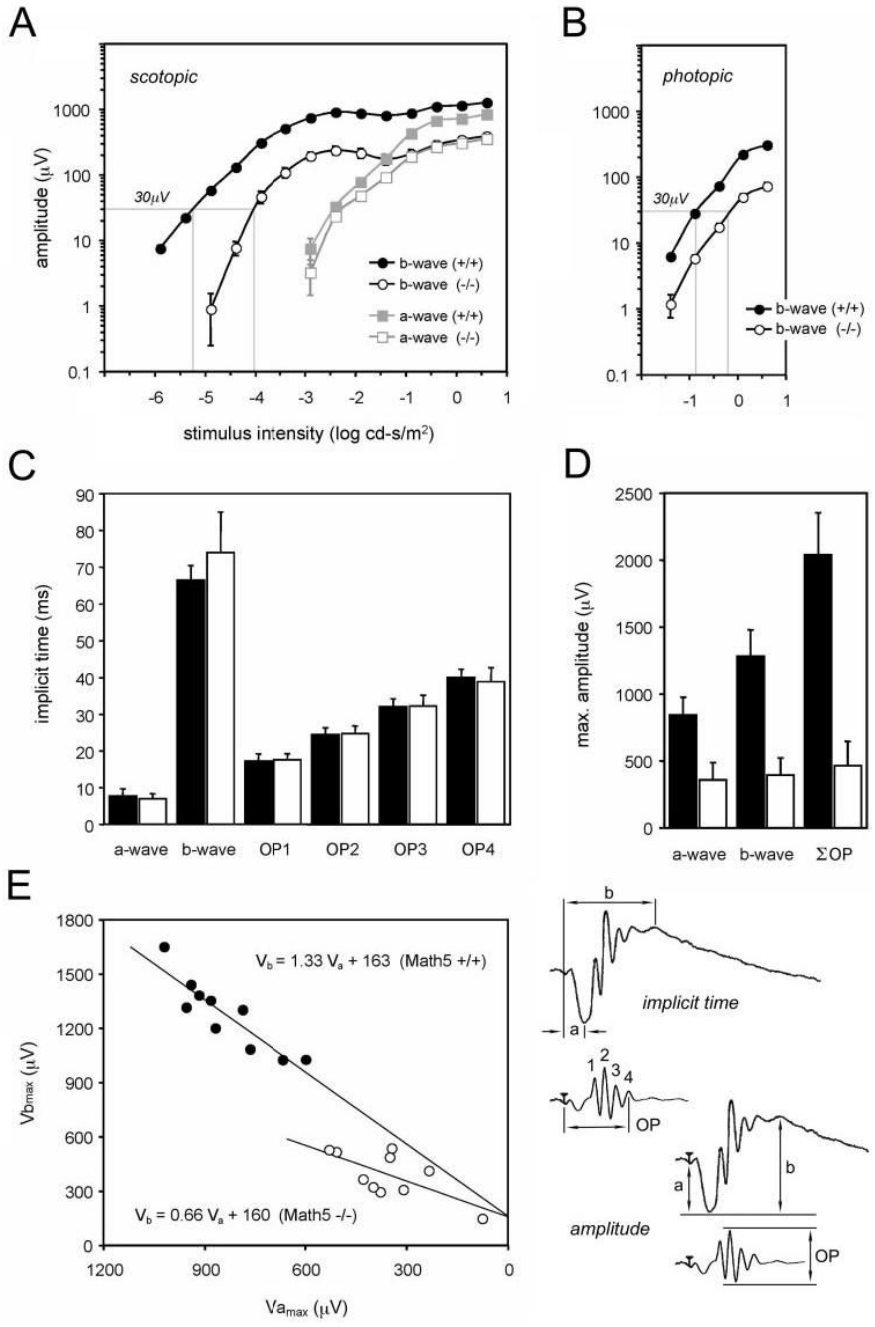

Figure 4.

Quantitative ERG analysis of wild-type and *Math5*-null mice. (**A**) Intensity vs. response (**V** − log **I**) plots for the scotopic b- and a-wave. (**B**) Intensity vs. response plots for the photopic b-wave. The intensity necessary to produce a 30-μV b-wave response is indicated in each panel by the *gray line* crossing the horizontal axis. The amplitudes are significantly reduced in *Math5*$^{-/-}$ retinas at all light intensities (*t*-test, **P* < 0.05), except for scotopic a-waves recorded at −2.4 and −2.9 log cd-s/m^2. Each point shows the average data recorded from 10 eyes (5 mice) ± SEM. (**C**) The implicit times for the scotopic a-, b- and OP waves recorded from wild-type (▪) and *Math5*$^{-/-}$ (□) mice at maximum stimulus intensity. (**D**) Comparison of a-wave, b-wave, and oscillatory potential amplitudes in wild-type (▪) and *Math5*$^{-/-}$ (□) mice. ∑OP is the

sum of the four largest oscillatory waves. The *bottom right* diagram shows how amplitudes and implicit times were measured. Error bars: SD. (**E**) Plot showing the altered relationship between scotopic maximum a-wave (Va_{max}) and b-wave (Vb_{max}) amplitudes in *Math5*$^{-/-}$ mice. Each symbol represents a different eye. The least-squares regression lines and equations are indicated. The b-wave was disproportionately reduced in the mutants. (○) *Math5*$^{-/-}$ (•) wild-type mice.

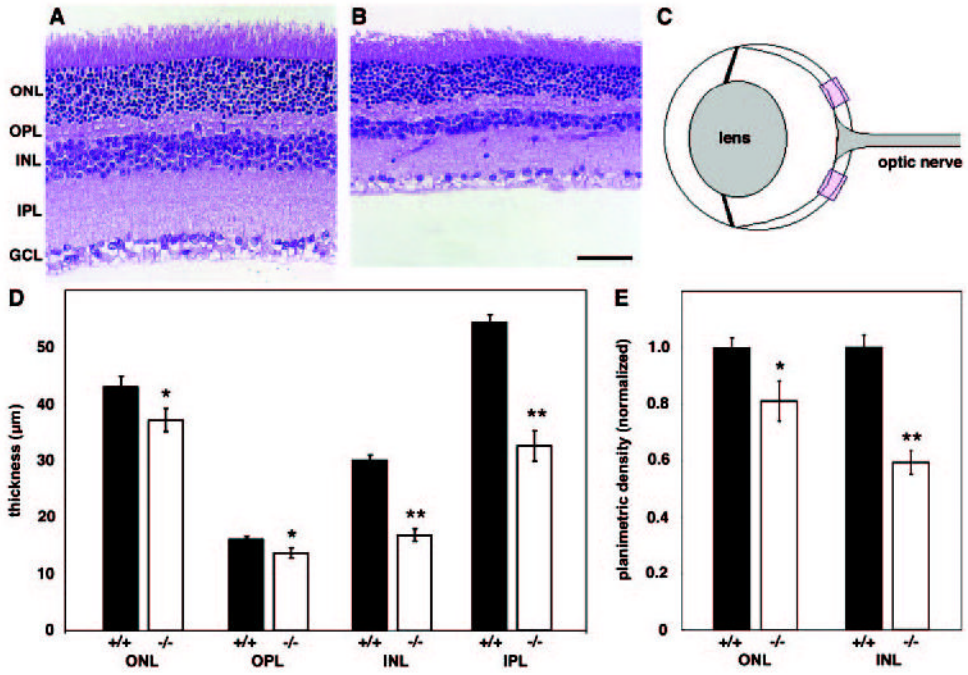

Figure 5.

Math5 mutant retinas have thinner nuclear and synaptic layers. Sections from wild-type (**A**) and *Math5*$^{-/-}$ (**B**) eyes were stained with H&E. The GCL is hypocellular due to the absence of RGCs. (**C**) Diagram showing 250-μm fields (*rectangles*) used for quantitative analysis of the retina. (**D**) Histogram comparing the thickness of wild-type (▪) and *Math5*$^{-/-}$ (□) retinal laminae. (**E**) Histogram comparing normalized planimetric cell density of wild-type (▪) and *Math5*$^{-/-}$ (□) ONL and INL. There were significantly fewer cells in the *Math5*$^{-/-}$ retinas, particularly within the INL. Scale bar, 50 μm; **P* < 0.05; ***P* < 0.001. Error bars, ±SEM.

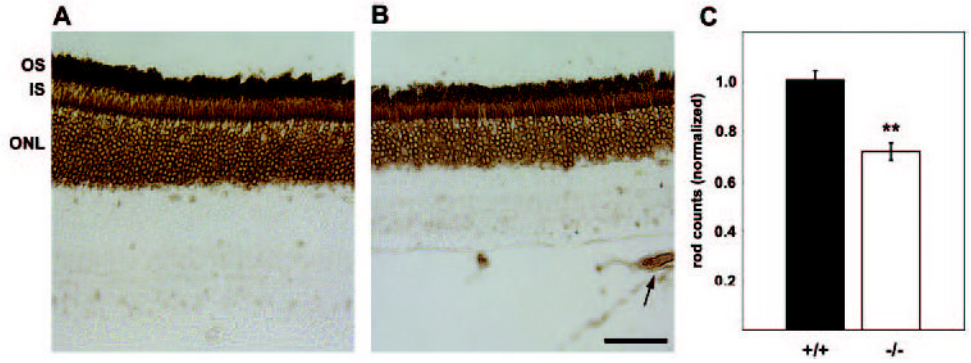

Figure 6.

Math5-null mice have fewer rods. Rod photoreceptors in wild-type (**A**) and *Math5*$^{-/-}$ (**B**) retinas were immunostained with RetP1, which labels rod outer (OS) and inner (IS) segments, and perikarya in the ONL. *Math5*$^{-/-}$ have persistent hyaloid vasculature (*arrow*) in the vitreous.[8] (**C**) Rod perikarya counts per field, normalized to wild-type. Scale bar, 50 μm; $^{**}P < 0.001$. Error bars, ±SEM.

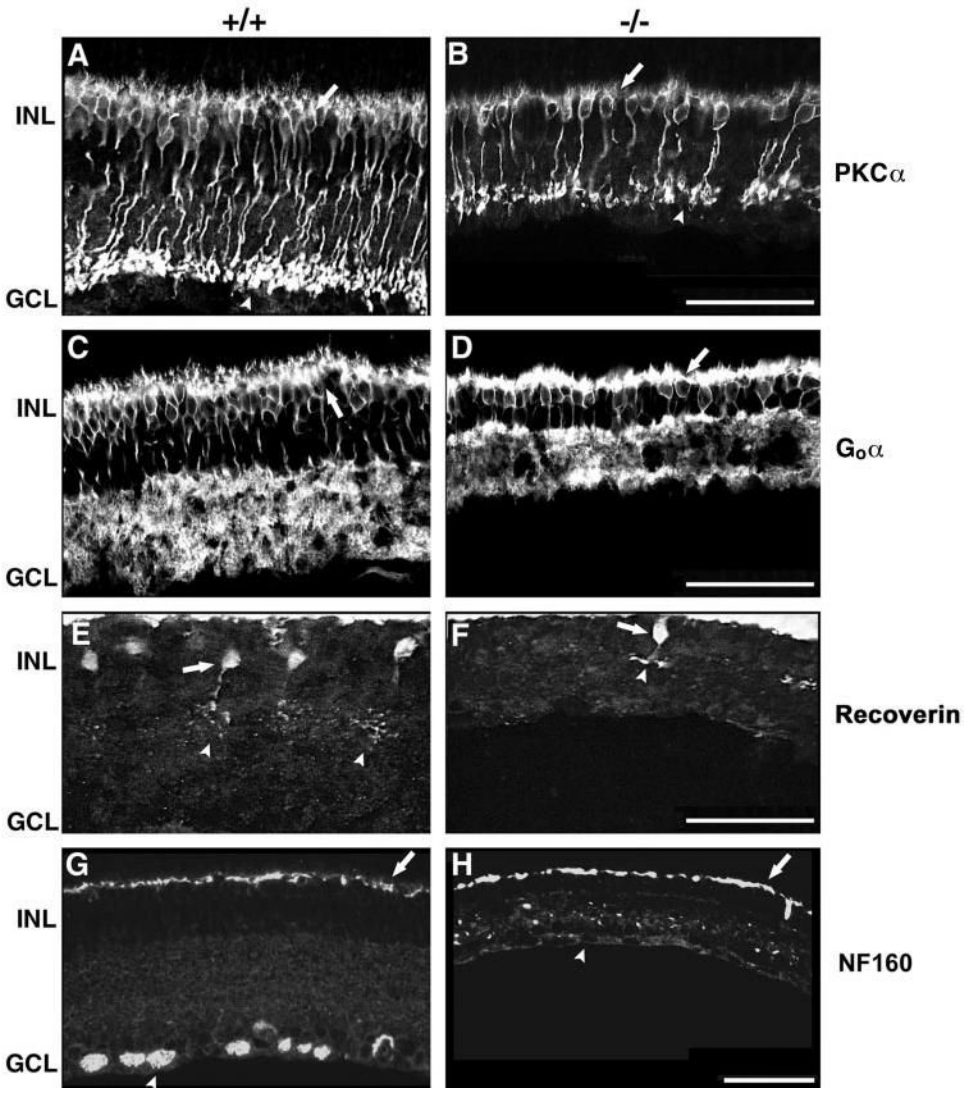

Figure 7.

Confocal immunofluorescence micrographs showing that all bipolar subtypes are decreased in *Math5* mutants. (**A**, **B**) PKCα staining of rod bipolar cells. Somata (*arrows*) and axon termini (*arrowheads*) are indicated. (**C**, **D**) $G_o\alpha$ staining of cone ON and rod bipolar cells. *Arrows*: $G_o\alpha$-positive somata. (**E**, **F**) Recoverin staining of cone OFF bipolar cells (*arrows*). Their axon termini are located in the OFF sublamina of the IPL (*arrowheads*). (**G**, **H**) Neurofilament 160-kDa staining of RGCs (*arrowhead*) and horizontal cells (*arrows*). The labeling of horizontal cells is equivalent in both retinas, but RGCs are absent in the *Math5*$^{-/-}$ animals. Scale bar, 50 μm.